Micro-objective manipulated with optical tweezers

doi: 10.1063/1.118260

Micro-objective manipulated with optical tweezers

Minoru Sasaki,[a] Tutomu Kurosawa, and Kazuhiro Hane
Department of Mechatronics and Precision Engineering, Tohoku University, Sendai 980-77, Japan

(Received 14 August 1996; accepted for publication 4 December 1996)

A microscope is described that uses a μm-sized ball lens, which is here termed micro-objective, manipulated with optical tweezers to image the side view of the arbitrary region of a sample. Since this micro-objective is small in size, it can go into a concave region to produce a local image of the inside which the conventional microscope cannot observe. Preliminary results show good lens performance from the micro-objective when combined with optical tweezers. © *1997 American Institute of Physics.* [S0003-6951(97)03306-8]

Conventional optical microscopes have been used due to their many advantages (e.g., easy to handle, noninvasive to samples). However, they are poor at investigating the side surface or inside of a hole or a narrow gap. There are hidden areas since the image is detected far from the sample using a microscope with a hard and bulky frame. To observe the inside, a small microscope (or at least imaging elements) which can go into the concave region of a sample would be useful. For this purpose, the microscope must be positioned and fixed stably during the measurement.

Among various manipulation techniques, optical tweezers is one of the promising methods for the damage-free position control of micro-particles,[1] and has been applied in various research fields.[2–5] When an incident laser beam is strongly focused on a transparent object having a refractive index larger than that of the surrounding medium, the total force of the radiation pressure acting on the object points in the neighborhood of the focal point, and the object is trapped there. The trapped particles are manipulated easily by scanning a microscope stage.

In this letter, we report on a microscope that uses a small lens as the objective. This micro-objective is made of a polystyrene sphere, and controlled to approach a specific area using optical tweezers. The locally magnified (or reduced) image of a surface is observed through the micro-objective.

The micro-objective used here is a $\sim$25 μm sized polystyrene particle. The μm-sized sphere can act as a ball lens.[6] As shown in Fig. 1, the sphere forms an image according to the lens equation:

$$\frac{1}{f}=\frac{1}{s}+\frac{1}{s'}, \tag{1}$$

where s and s' is the distance between the object and the micro-objective, and between the micro-objective and the projected image, respectively, f is the focal length of the micro-objective as given by

$$\frac{1}{f}=\left(\frac{n_1}{n_2}-1\right)\frac{2}{r}, \tag{2}$$

n_1 and n_2 are the refractive index of the polystyrene (1.59) and that of the surrounding water (1.33), respectively, and r is the radius of the micro-objective. A micro-objective of 25 μm diameter has a focal length of 32 μm. The focal point is outside the sphere in our experiments.

[a]Electronic mail: sasaki@hane.mech.tohoku.ac.jp

The position of the image surface and the magnification are dependent on the geometry of the object and the micro-objective. If the object is farther than the focal length, the micro-objective makes a real image, as shown in Fig. 1(a). If nearer, a virtual image is generated, as shown in Fig. 1(b). The virtual image is opposite in direction to the real image. An eyepiece further projects these images onto the monitor screen.

Figure 2 shows the experimental setup. The system consists of two coupled microscopes. One is aligned vertically to observe a top view of the sample as well as to trap the micro-objective. The other is aligned laterally to observe a side view using the micro-objective. The trapping light source is a laser diode (Sony, model SLU303XR, 830 nm, $<$400 mW). The laser beam is focused by the objective (Olympus, 50$\times$, numerical aperture [NA] = 0.55, working distance $=\sim$9 mm) of the vertical microscope. The trapped micro-objective is carried close to a specific region of the sample being observed, and the top view is displayed using a charge coupled device (CCD) camera and video monitor (monitor$_1$). The side view is observed simultaneously through the lateral microscope, which uses another CCD camera and video monitor (monitor$_2$). The eyepiece (Olympus, 20$\times$, NA = 0.40, working distance = $\sim$11 mm) is aligned to image the viewing plane of the micro-objective by moving the base stage. Each microscope uses a halogen lamp for illumination.

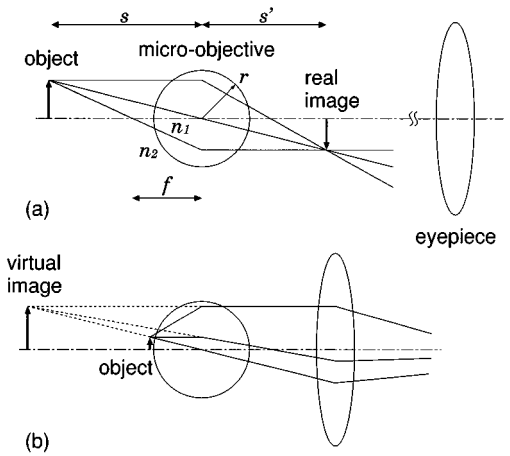

FIG. 1. Schematic diagram to explain the lens function of the micro-objective. There are two cases where the micro-objective generates (a) the real image and (b) the virtual one.

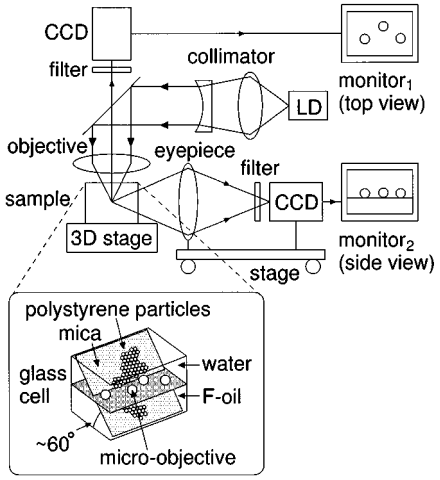

FIG. 2. Schematic diagram of the experimental setup to detect the side view through the micro-objective. The illumination lamps and condenser lenses are not shown. The distance between the eyepiece and the CCD camera of the lateral microscope is fixed at ~30 cm. Before each series of experiments, the optical alignment is adjusted so that the two monitors observe the same position. The astigmatism of the laser diode (LD) beam weakens the trapping force.

The inset of Fig. 2 shows the sample glass cell placed on a three-dimensional stage. The glass cell is $1\times2\times1\text{cm}^3$ in dimensions, and the glass walls are 2 mm in thickness. The spatial pattern to be imaged by the micro-objective was the partially distributed array of smaller polystyrene particles (diameter = 2.02 μm) on a mica substrate.[7] For a stronger adhesion of the array to the mica substrate, the polystyrene particles were slightly heated to melt only at the surface keeping their spherical shape. This mica substrate was oriented at an angle of ~60° to the horizontal in the cell so as not to disturb the path of the trapping laser beam. At first, F-oil (perfluoromethyldecalin, refractivity = 1.32, density =1.94 g/cm^3) was poured into the cell until its surface

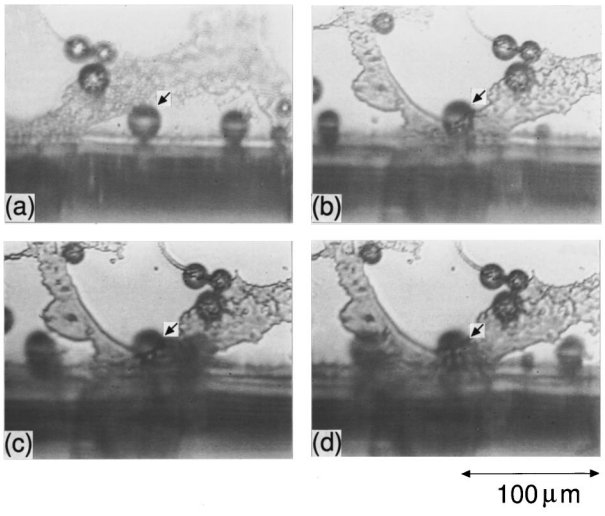

FIG. 3. A series of monitor images showing the micro-objective together with the image of the background array of smaller particles. (a) The initial configuration of the sample. (b) The micro-objective is moved laterally to the area of interest. (c) The image is further magnified by moving the micro-objective nearer to the particulate array. (d) The magnified image when the micro-objective is moved a little to the right. The spherical aberration of the micro-objective somewhat distorts the image.

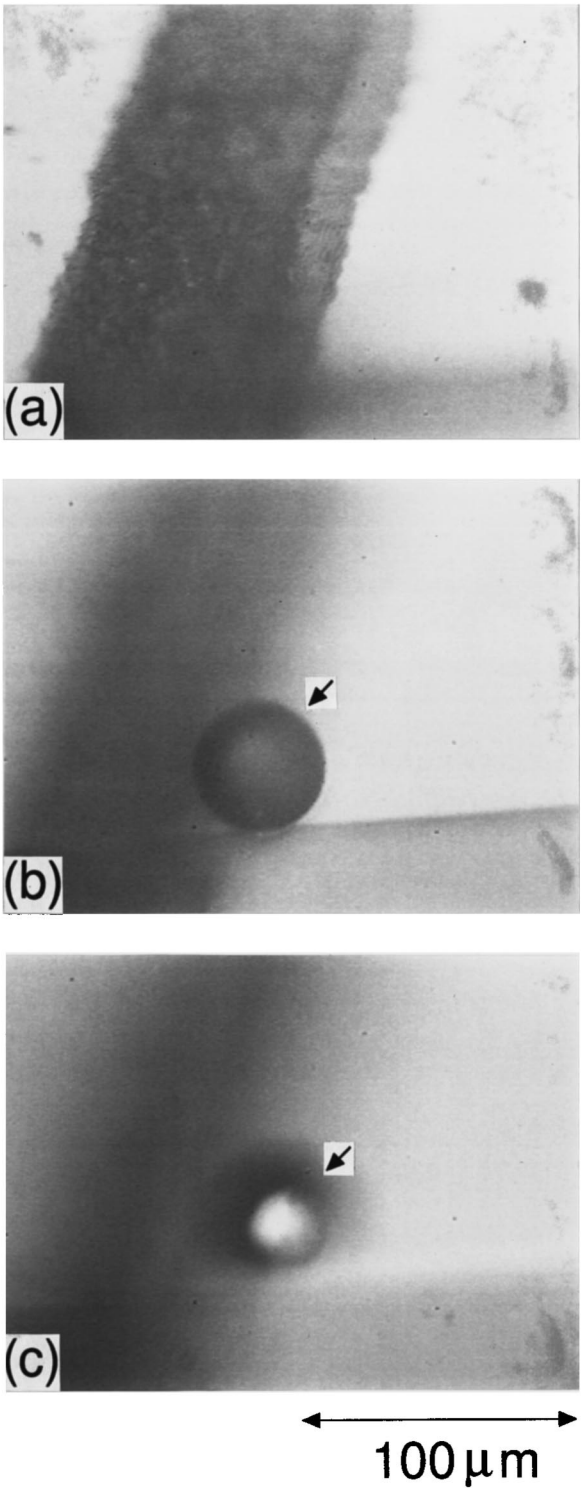

FIG. 4. The monitor screens showing the configuration of (a) the sample and (b) the micro-objective. (c) The reduced image of the background belt of the particulate array is shown in the right half of the micro-objective.

reached the appropriate height. Next, the cell was filled with distilled water. To form an interface between F-oil and water horizontal, an appropriate surfactant was added to the F-oil. A few drops of solution including the micro-objective were pipetted into the cell. Since micro-objectives (density = 1.06 g/cm^3) are heavier than water and lighter than F-oil, they stay on the interface between F-oil and water.

Figure 3 is a series of side views. The darker lower half

of the micrograph corresponds to the F-oil region. The arrows indicate the trapped micro-objective, which is confirmed by the brilliant light of the trapping laser beam scattered on the micro-objective observed when the infrared blocking filter is removed. Figure 3(a) shows the initial configuration. Using the optical tweezers, the micro-objective is carried from right to left while the other particles stay at their initial positions. In Fig. 3(b), the image of smaller particles in the background array is apparent inside the micro-objective. The particles are slightly magnified by the micro-objective. To magnify the image further, the micro-objective is manipulated to approach the array perpendicularly to the paper. Figure 3(c) shows an image of three particles at higher magnification. Individual particles can be seen, in contrast to the unresolved image observed without the micro-objective. The magnification of the micro-objective is $\sim 5\times$. Since the micro-objective can be moved close to the area of interest, its NA can be large. Figure 3(d) shows the image when the micro-objective is moved a little to the right. The displacement of the image is seen to be larger than the movement of the micro-objective. When a virtual image is formed by the micro-objective, it moves in the opposite direction to the displacement of the micro-objective. Although it is difficult to see in the stationary pictures, the image spreads over a larger area than the cross-section of the micro-objective. The bright background hides the outer portion of the image.

Figure 4 shows the case where a reduced image is observed. In Fig. 4(a), the vertical belt is the particulate array and the micro-objective is far from the sample. Figure 4(b) shows the relative position of the micro-objective. Figure 4(c) shows the image made by the micro-objective. The reduced image of the array is evident inside the micro-objective and is reversed in direction. The darker right half of the micro-objective corresponds the particulate array. The observed real image does not correspond to the area just behind the micro-objective due to the imperfect alignment of the lateral microscope. This image moves in the same direction to the displacement of the micro-objective, and the speed of the image is slower than that of the micro-objective. These behaviors show that the image is a real one.

In conclusion, the lens function of the micro-objective is usefully combined with the optical tweezers manipulation technique to constitute a unique microscope. A magnified (or reduced) side view of an arbitrary region of the sample is locally observed.

The microscope objectives ($50\times$ and $20\times$) with ultra-long working distances were kindly provided by Y. Bessho, R&D Center, Brother Industries Corp.

[1] A. Ashkin, Phys. Rev. Lett. **24**, 156 (1970).
[2] A. Ashkin, Science **210**, 1081 (1980).
[3] A. Ashkin, J. M. Dziedzic, and T. Yamane, Nature **330**, 769 (1987).
[4] N. Tamai, T. Asahi, and H. Masuhara, Rev. Sci. Instrum. **64**, 2496 (1993).
[5] H. Misawa, R. Fujisawa, K. Sasaki, N. Kitamura, and H. Masuhara, Jpn. J. Appl. Phys. 1 **32**, L788 (1993); K. Sasaki, H. Misawa, N. Kitamura, R. Fujisawa, and H. Masuhara, *ibid.* **32**, L1144 (1993).
[6] S. Hayashi, Y. Kumamoto, T. Suzuki, and T. Hirai, J. Colloid Interface Sci. **144**, 538 (1991).
[7] A. S. Dimitrov, C. D. Dushkin, H. Yoshimura, and K. Nagayama, Langmuir **10**, 432 (1994).